A MICROMACHINED FLUIDIC REDUCED INERTIAL MEASUREMENT UNIT USING THERMAL EXPANSION FLOW PRINCIPLE

S.S. Wang[1], X.H. Gong[1], B. Nie[1], W.Z. Yuan[1], and H.L. Chang[1]*
[1]MOE Key Laboratory of Micro and Nano Systems for Aerospace, Northwestern Polytechnical University, Xi'an, China

ABSTRACT

This paper presents a micromachined fluidic integrated reduced inertial measurement unit based on the thermal expansion flow principle. The proposed multi-axis gas sensor can achieve the simultaneous detection of single-axis (Z-axis) angular rate and dual-axis (X-axis and Y-axis) acceleration using one chamber. To the best of the authors' knowledge, it is the first time that such a multi-axis thermal expansion flow inertial sensor is reported. A large measurement range has been demonstrated, e.g., the Z-axis gyroscope can achieve a sensitivity of 0.548 mV/°/s with a nonlinearity less than 3.87% within the input range of ±2160 °/s.

KEYWORDS

Thermal expansion flow, multi-axis gas sensor, gyroscope, accelerometer, thermistor

INTRODUCTION

Over the past twenty five years, various micromachined inertial sensors have emerged. Most of them use one or two solid proof masses suspended by different mechanical springs to detect the acceleration or angular rate [1-2]. However, this kind of the mechanical inertial sensors would give rise to some inherent problems after long operating time such as structural fatigue, low shock resistance and vibration noise [3]. Recently, some inertial sensors using the fluid medium instead of the solid proof mass to detect the acceleration or angular rate [4-7].

Zhu et al. reported a micromachined fluidic inertial senor based on natural convection which has a relative simple structure including a suspended central heater and four suspended thermistor wires to achieve detection of the Z-axis angular rate and X/Y-axis acceleration [4]. However, the sensor's sensitivity is limited by the earth's gravity field. The sensitivities can be improved by using forced-convection instead of the natural convection [5-7]. However, the forced convection need to be generated by various micro-pumps, which restricts the miniaturization of the inertial sensors.

Leung et al. [8] reported a thermal expansion-flow microgyroscope using a bidirectional gas motion generated by heaters, which successfully avoids of the usage of the micro-pumps. Cai et al. [9] presented a similar sensor which can sense one-axis angular rate and one–axis acceleration. In the both works [8-9], the platinum (Pt) is used as the thermistor. However, the resistance uniformity of Pt is not as good as silicon, which may affect the linearity of the scale factor. In this paper, we improved the thermistor by using p-type silicon as the sensing element, which has a higher temperature coefficient of resistance (TCR) value and a better uniformity than Pt. Thus the sensitivity of the sensor can be increased. More importantly, we use a new design scheme, thus the gas sensor can simultaneously sense Z-axis angular rate and dual-axis (X-axis and Y-axis) acceleration (sometimes this multi-axis sensor is called as a reduced IMU [10]). A silicon-on-insulator (SOI) process is proposed to fabricate the thermistors, which has been validated to have good resistance uniformity.

WORKING PRINCIPLE

The configuration of the multi-axis sensor is schematically depicted in Figure 1. The core of the sensor is a silicon sensing chip packaged in a hermetic chamber filled with air. The sensing chip is formed by four heaters at the center surrounded by eight identical thermistors. In order to generate the continuous thermal expansion flow, the heaters are driven by a square wave. In the absence of rotation or linear acceleration, the temperature profile inside the chamber will be symmetrical, thus the temperature on the thermistors are the same, as shown in Figure 2(a).

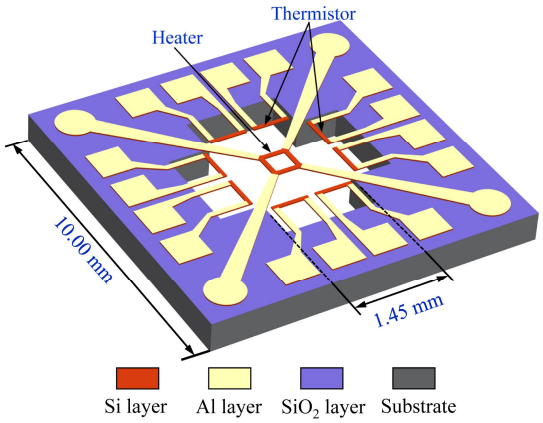

Figure 1: Configuration of the multi-axis inertial sensor.

When an angular rate about the Z-axis is applied, the Coriolis effect causes the gas flow to deflect from the symmetrical path and causes an opposite temperature change between R_{x1} and R_{x2}, R_{x4} and R_{x3}, R_{y1} and R_{y2}, and R_{y4} and R_{y3}, as illustrated in Figure 2(b). The total temperature changes can be calculated as follows:

$$\Delta T_{GyroZ} = T(R_{x2}) - T(R_{x1}) + T(R_{x3}) - T(R_{x4}) + T(R_{y2}) - T(R_{y1}) + T(R_{y3}) - T(R_{y4}) \quad (1)$$

where $T(R_i)$ is the temperature of the thermistor R_i, and the

subscript *i* denotes one of the eight thermistors.

Due to the thermoresistive effect, the resistances of the eight thermistors change, and are converted to the voltage output by the corresponding Wheatstone bridges. The output voltage can be expressed as follows [6], [11]:

$$V_{OUT-\omega_Z} = \frac{\alpha \Delta T_{GyroZ}}{4} \cdot V_{cc} \tag{2}$$

where α and V_{cc} are the TCR of the thermistor and the supply voltage of the Wheatstone bridge, respectively.

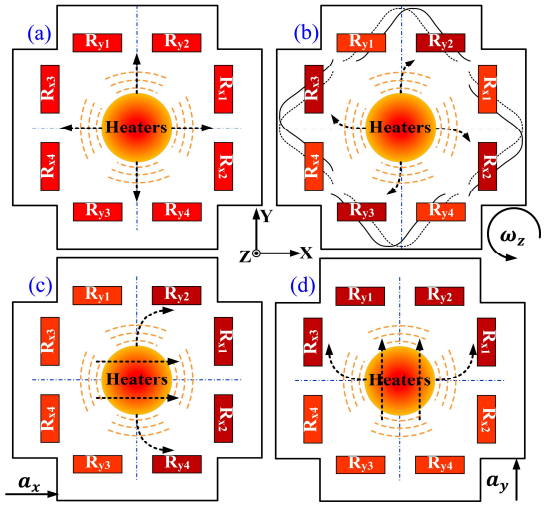

Figure 2: Conceptual operating principle of the thermal sensor; (a) In the absence of rotation or acceleration, hot gas flows symmetrically move from the heaters to the thermistors; (b) The gas flows deflect from the symmetrical path in the presence of Z-axis angular rate; (c) (d) The gas flows move in the direction of the applied acceleration in the presence of X/Y-axis linear acceleration.

When an X-axis linear acceleration is applied, the gas flow moves in the direction of the applied acceleration, causing an opposite temperature change between the R_{x1} and R_{x3}, R_{x2} and R_{x4}, R_{y2} and R_{y1}, and R_{y4} and R_{y3}, as illustrated in Figure 2(c). Thus, the total temperature changes can be calculated as follows:

$$\begin{aligned} \Delta T_{AccX} = {} & T(R_{x1}) - T(R_{x3}) + T(R_{x2}) - T(R_{x4}) + \\ & T(R_{y2}) - T(R_{y1}) + T(R_{y4}) - T(R_{y3}) \end{aligned} \tag{3}$$

Similarly, as illustrated in Figure 2(d), the total temperature change induced by Y-axis linear acceleration can be calculated as follows:

$$\begin{aligned} \Delta T_{AccY} = {} & T(R_{y1}) - T(R_{y3}) + T(R_{y2}) - T(R_{y4}) + \\ & T(R_{x1}) - T(R_{x2}) + T(R_{x3}) - T(R_{x4}) \end{aligned} \tag{4}$$

The resistance changes of the eight thermistors induced by X/Y-axis linear acceleration can be converted to the voltage output according to the corresponding Wheatstone bridges, and output of the bridge can be written as follows:

$$V_{OUT-a_{x/y}} = \frac{\alpha \Delta T_{Acc\,X/Y}}{4} \cdot V_{cc} \tag{5}$$

For achieving the simultaneous detection of single-axis (Z-axis) angular rate and dual-axis (X-axis and Y-axis) acceleration, we design the read-out circuits including four Wheatstone bridges, as shown in Figure 3.

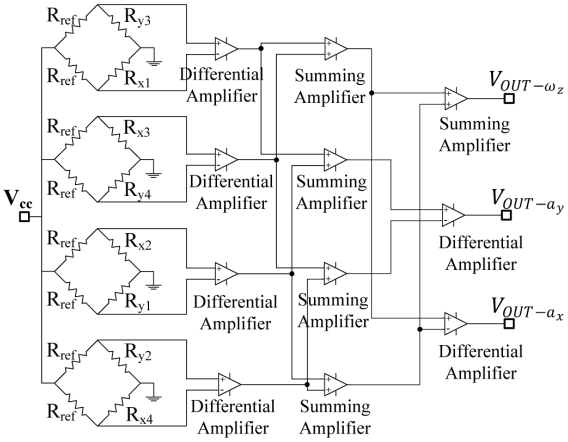

Figure 3: Schematic diagram of the read-out circuit of the eight thermistors. R_{ref} is the reference resistor for balancing the Wheatstone bridges.

SIMULATIONS

For the gas sensor, it is of vital importance to arrange the sensing element into a proper position in the detection chamber for achieving high sensitivity [5], [11]. In this research, a numerical simulation was used to investigate where the thermistors should be placed to achieve the high sensitivity.

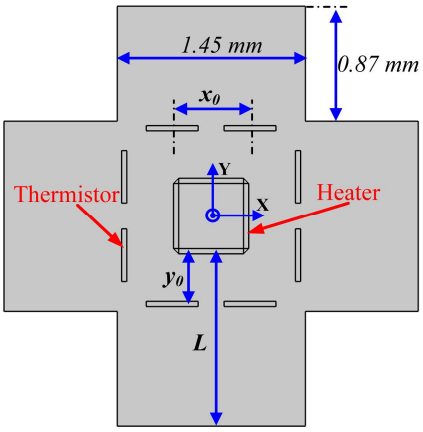

Figure 4: The 2-D fluidic model of the gas sensor. Air is selected as the gas working medium.

A transient two-dimensional model was constructed and meshed to investigate the gas flow in the chamber using the commercial software COMSOL Multiphysics, as shown in Figure 4. The gas flow in the hermetic chamber was modeled as the Newtonian fluid undergoing a compressible laminar flow.

In the simulation, the heaters receive a 20 Hz square

wave, and its power is 70 mW. Meanwhile, a Z-axis angular rate of 10 rad/s is applied in this model. Figure 5 shows the temperature differences induced by Z-axis angular rate at the various positions of the thermistors in the chamber. Simulation results indicate that the temperature difference ΔT_{GyroZ} can achieve a high value more than 0.4 K, when the position of the thermistor meet the parameters as follows:

$$0.13 \le y_0/L \le 0.30 \quad (6)$$

$$0.59 \le x_0 \le 0.76 \quad (7)$$

where y_0, L and x_0 are respectively the distance from the heater to the thermistor, the distance from the heater to the cavity wall and the distance between two adjacent thermistors at each end of the cavity.

When the location y_0/L=0.28 and x_0=0.74 mm is selected as the position of the thermistor, the temperature differences under Z-axis angular rate and the X/Y-axis linear acceleration are shown in Figure 6(b) and Figure 6(c), respectively. Figure 6 illustrates that the induced temperature differences under Z-axis angular rate and X/Y-axis linear acceleration are periodic temperature fluctuations with the heaters switching on and off alternately.

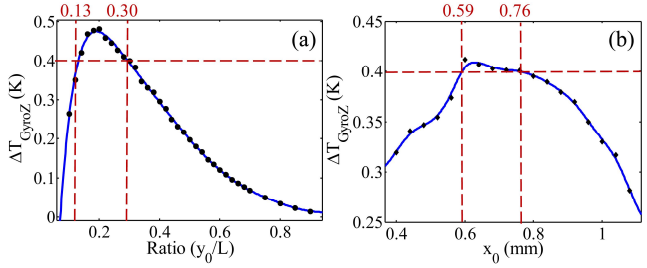

Figure 5: (a) The change of ΔT_{GyroZ} with the variation of the ratio (y_0/L) under an applied Z-axis angular rate of 10 rad/s; (b) The change of ΔT_{GyroZ} with the variation of x_0 under an applied Z-axis angular rate of 10 rad/s.

FABRICATION PROCESS

The SEM graph of the sensing chip is shown in Figure 8(b). The fabrication of the sensing chip begins with a SOI wafer with a 30-μm-thick p-type device layer, 1.5-μm-thick buried oxide and 400-μm-thick handle layer (Figure 7(a)). Next, the backside of the wafer is patterned by photolithography, and the plus-shaped-cavity is formed by ICP etching on handle layer and BOE etching on SiO_2 (Figure 7(b)). Aluminum (Al) anchors of 200 nm in thickness for interconnection are created by sputtering, photolithography and Al etching. Then, rapid thermal annealing is carried out to enhance the ohmic contact between the Al anchors and the device layer (Figure 7(c)). Next, the device layer is patterned by photolithography, and the thermistors are formed by ICP etching (Figure 7(d)). Then, the fabricated sensing chip is aligned and bonded on the PCB board, as shown in Figure 8(a). The anchors of the thermistors are connected to the anchors on the PCB board through aluminum-silicon bonding wire. The chip is sealed with a PMMA cap, and the chamber is filled with air at a pressure of 1 atm. A prototype of the packaged device is shown in Figure 8(c).

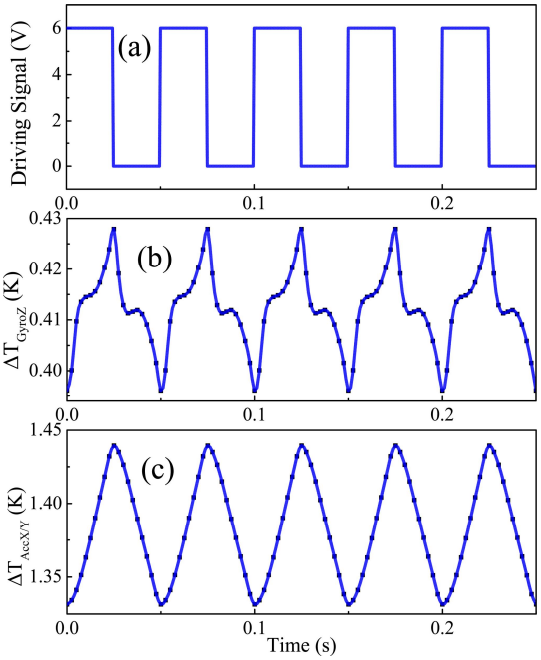

Figure 6: (a) Driving signal of the heaters; (b) Simulated difference signal of applying 10 rad/s angular rate about the Z-axis; and (c) Simulated difference signal of applying 1g X-axis (Y-axis) linear acceleration.

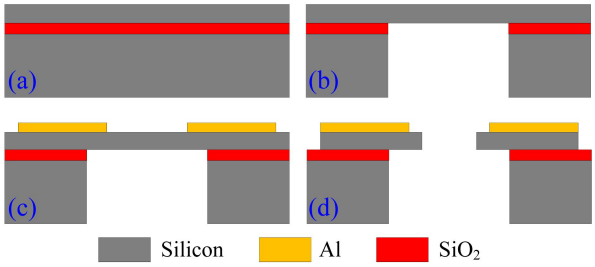

Figure 7: Fabrication process flow for the sensing chip.

EXPERIMENTS

The rotation measurements are performed using a rotation table with an error less than 0.001 °/s. As indicated in Figure 9, the measured sensitivity of the Z-axis gyroscope is 0.548 mV/°/s with a nonlinearity less than 3.87% in the range of ±2160 °/s. The acceleration measurements are conducted using a rotary dividing table with an uncertainty of ±0.1° in the readings. The measured sensitivities of the accelerometer of the X-axis and Y-axis are 0.309 V/g and 0.305 V/g, respectively, as shown in Figure 10.

The above results of the experiment are obtained using an amplification gain of 4000. All the experimental data in this section are acquired under the heaters driven by a 9 V, 20 Hz, 50% duty cycle square wave signal.

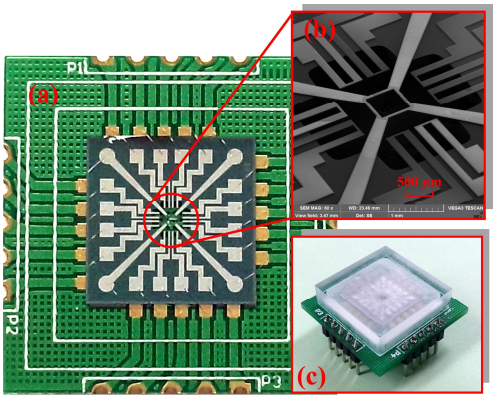

Figure 8: (a) A prototype of unpackaged device; (b) SEM of the sensing chip central area; and (c) prototype of a packaged device.

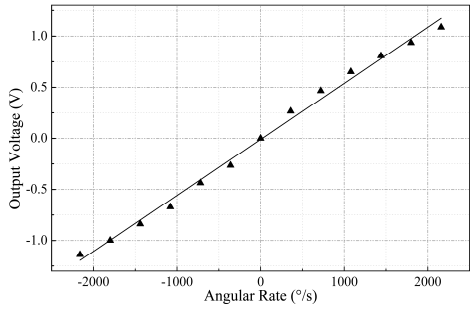

Figure 9: Output voltage of the Z-axis gyroscope versus applied angular rate.

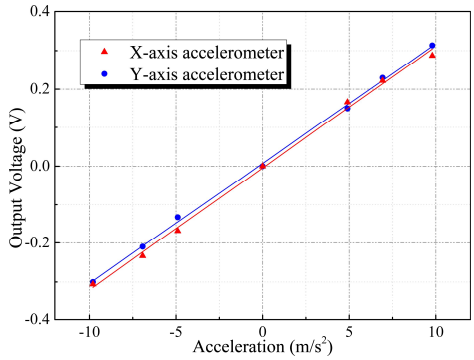

Figure 10: Output voltage of the X/Y-axis accelerometer versus applied acceleration.

CONCLUSIONS

This paper reports a multi-axis inertial sensor based on thermal expansion principle. In addition to the advantages of simple structure, low fabrication cost and high shock resistance, the sensor also presents the advantage of large measurement range rotation with good linearity.

ACKNOWLEDGEMENTS

The work was supported in part by the National Natural Science Foundation of China under Grant 61273052, in part by the National Key Scientific Instrument and Equipment Development Projects of China under Grant 2013YQ04091102, in part by the Fundamental Research Funds for the Central Universities under Grant 3102014JC02010505 and in part by the 111 project under Grant B13044.

REFERENCES

[1] N. Yazdi, F. Ayazi, K. Najafi, "Micromachined inertial sensors," *Proc. IEEE*, vol. 86, no. 8, pp. 1640–1659, Aug. 1998.

[2] D. Xia, C. Yu, L. Kong, "The development of micromachined gyroscope structure and circuitry technology," *Sensors*, vol. 14, no. 1, pp. 1394-1473, Jan. 2014.

[3] M. Weinberg, A. Kourepenis, "Error sources in in-plane silicon tuning-fork MEMS gyroscopes," *J. Microelectromech. Syst.*, vol. 15, no. 3, pp. 479-491, Jun. 2006.

[4] R. Zhu, Y. Su, H. Ding, "A MEMS hybrid inertial sensor based on convection heat transfer," in *Proc. 13th Int. Conf. Solid-State Sensors, Actuat., Microsyst. (Transducers)*, Seoul, Korea, Jun. 2005, pp. 113–116.

[5] H. Chang, P. Zhou, J. Xie, X. Gong, Y. Yang, and Z. Yuan, "Theoretical modeling for a six-DOF vortex inertial sensor and experimental verification," *J. Microelectromech. Syst.*, vol. 22, no. 5, pp. 1100–1108, Oct. 2013.

[6] H. Chang, X. Gong, S. Wang, P. Zhou, W. Yuan, "On improving the performance of a triaxis vortex convective gyroscope through suspended silicon thermistors", *IEEE Sensors Journal,* vol. 15, no. 2, pp. 946-955, Sep. 2014.

[7] V. Dau, V. Dzung, T. Shiozawa, S. Sugiyama, Simulation and fabrication of a convective gyroscope, *IEEE Sensors Journal,* vol. 8, no. 9, pp. 1530-1538, Sep. 2008.

[8] J. Bahari, R. Feng, A. Leung, "Robust MEMS gyroscope based on thermal principles," *J. Microelectromech. Syst.*, vol. 23, no. 1, pp. 100-116, July. 2013.

[9] S. Cai, R. Zhu, H. Ding, J. Yong, Y. Su, " A micromachined integrated gyroscope and accelerometer based on gas thermal expansion", in *Proc. 17th Int. Conf. Solid-State Sensors, Actuat., Microsyst. (Transducers),* Barcelona, Spain, June 16-20, 2013, pp. 50-53.

[10] H. Chang, J. Xie, Q. Fu, Q. Shen, W. Yuan, "Micromachined inertial measurement unit fabricated by a SOI process with selective roughening under structures," *Micro & Nano Letters*, vol. 7, pp.486-489, 2011.

[11] V. Dau, D. Dao, S. Sugiyama, "A 2-DOF convective micro accelerometer with a low thermal stress sensing element," *Smart Material & Structures*, vol. 16, no. 6, pp. 2308-2314, Dec. 2007.

CONTACT

*H.L. Chang, tel: +86-29-88492841; changhl@nwpu.edu.cn